Network Constrained Economic Dispatch of Integrated Heat and Electricity Systems through Mixed Integer Conic Programming

Huang, Shaojun; Tang, Weichu; Wu, Qiuwei; Li , Canbing

Published in:
Energy

Link to article, DOI:
10.1016/j.energy.2019.05.041

Publication date:
2019

Document Version
Early version, also known as pre-print

Network Constrained Economic Dispatch of Integrated Heat and Electricity Systems through Mixed Integer Conic Programming

Shaojun Huang [a,*], Weichu Tang [b], Qiuwei Wu [c], Canbing Li [d]

[a] *Center for Energy Informatics, Mærsk Mc-Kinney Møller Instituttet, University of Southern Denmark, Denmark*
[b] *CITIC Construction Co.,Ltd, Chaoyang District, Beijing, China*
[c] *Center for Electric Power and Energy, Department of Electrical Engineering, Technical University of Denmark, Denmark*
[d] *College of Electrical and Information Engineering, Hunan University, Changsha, China*

Abstract

This paper proposes an economic dispatch method for an integrated heat and electricity system with respect to network constraints. Network constraints are usually nonlinear and can cause severe difficulties for optimization solvers. Particularly, in a heating network, the mass flow mixing at each node and the pressure and temperature drop along each pipe involve both hydraulic and thermal processes, which can cause high nonlinearity that has not been properly modeled. This paper will firstly model the power and heat network constraints by using a nonlinear model, which is accurate but hard to solve. Then, simplification and convexification will be employed to reform the nonlinear constraints to linear and conic ones. Consequently, the entire economic dispatch problem will be modeled as a mixed integer conic programming problem. Because the proposed model allows for the changes of the mass flow rate and direction, an optimal mass flow profile can be achieved along with the solution of the economic dispatch. Case studies on an integrated district heating and power system with a portfolio of power and heat sources show that the proposed economic dispatch model can handle the complexity of the network constraints and make optimal dispatch plans for multi-energy systems.

Keywords: integrated heat and electricity system; district heating network; combined heat and power (CHP); economic dispatch; multi-energy systems (MES); mixed integer conic programming (MICP)

Nomenclature

Sets

N_t	set of time periods for planning

Key Parameters

A	node to pipe incidence matrix
A^+, A^-	positive/ negative elements of A
B	heat sources to heat nodes incidence matrix
D	Power transfer distribution factor (PTDF)
L	length of each pipe (m)
M	a large number, e.g., 99999.9
K	pipe hydraulic resistance coefficient
b	cost coefficient of energy sources
c_t	system price of the external grid
c_p	heat capacity of the mass flow
$p^{\max}$	maximum active power of energy source
π	heat / power ratio of CHP/boiler/heat pump
λ	heat transfer coefficient of pipes
θ_0	initial heat energy level of HA
θ'_0	initial SOC level of a battery

*Corresponding author. Address: Campusvej 55, 5230 Odense M, Denmark. Email: shahu@mmmi.sdu.dk

Key Variables	
$T_{s,t}$	supply temperature of each node
T_r	return temperature of each node
$T_{sm,t}$	mixed temperature of the supply network
$T_{rm,t}$	mixed temperature of the return network
u^+, u^-	inlet / outlet temperature of each pipe (supply network)
v^+, v^-	inlet / outlet temperature of each pipe (return network)
m_t	mass flow injection of each node
x_t	mass flow rate of each pipe
P	line flow of the power system
p	output power (p_g — CHP, p_{pv} — PV)
$p_{0,t}$	power imported from the external grid
y	binary variable, indicating the actual mass flow direction of each pipe
Φ	heat power injection of each node
ρ	pressure level of each node
κ_t	pressure loss of pipes
ϕ	heat output of each heat source
θ_t	heat energy level of HA
θ'_t	SOC level of a battery

1. Introduction

The overall goal of the energy sector in Denmark is that the entire energy sector should be 100% based on renewable by 2050, of which district heating will play a substantial role [1]. There are many challenges towards this goal, especially the difficulties in the management of the uncertainties and intermittency of renewable production. To handle these challenges, more flexibilities are needed. This means more battery storages, more flexible demands, etc. Integrating district heating (DH) with a power system and the co-optimization/co-dispatch of such an integrated system are very important aspects among others that are worthy to investigate. The integrated system, named as a “multi-energy system” (MES), can offer more flexibilities than separated systems.

Like a distribution grid for supplying electricity to end users, DH is a system for distributing heat through a system of insulated pipes for residential and commercial heating requirements. The district heating technologies and the economics from the investment point of view are reviewed in [2]. District heating and power systems are connected in many ways, through e.g., combined heat and power (CHP) plants, electric boilers and/or heat pumps. The 4th generation district heating technology [3] will use low-temperature heat carrier systems, which will call for the use of electric heat boosters at the premises of the end users [4] — evidence that shows the potential connection between district heating and power systems.

The modeling and optimization of an MES is a challenging task. The heating part is more challenging because the power part has been well modeled in many previous works, including the following references. Pan et al. [5] have studied an MES and proposed an algorithm which can analyze the interactions of different sectors of the MES. This MES was modeled through nonlinear models and solved by Newton methods with back-and-forth iterations between the power and the heating systems. Liu etc. [6] have studied an MES with a gas system included. Instead of back-and-forth iterations, the authors of [7] proposed a combined analysis method through a large model covering both heating and power systems. Dong et al. [8] have introduced a

state estimation method to an MES, which has already been widely used in power systems. Furthermore, [9] proposed a two-stage state estimation method for the analysis of an MES, which considered the longer time delay of DH systems compared to power systems. However, all these methods did not consider optimization.

A plant-level optimization tool was developed in [10] for optimal operation of CHP plants. Chen et al. [11] have investigated an optimal operation method and applied to CHP plants in order to provide extra flexibility for the wind power integration in China. Resource optimization methods were applied on combined heat and power microgrids [12]. Dimoulkas etc. [13] have proposed a stochastic optimization method for the scheduling of CHP plants with uncertain electricity prices and heat demands. Furthermore, [14] proposed a stochastic programming method for the co-dispatch of CHP plants and wind power, which considered a short-term wind power forecast. All these works focused on the co-dispatch of multiple energy sources, but did not consider the limitation of the networks that might make it impossible to transfer the desired power from these sources to customers or load centers. For instance, congestion in power systems can affect the power transfer and result in different locational marginal prices [15]. Likewise, congestion in heating systems due to limited pump capacity and/or temperature regulation requirements can also limit the amount of heat power from certain locations that can be delivered to end users.

The optimization models for a whole MES, including the sources and the networks, have been studied in many previous works as well. The very early work on this subject was described in [16], but this system has heating only and only one heat plant to dispatch. In its model, the supply temperature of the heating network is optimized. Although the entire model is a nonlinear model, the optimal temperature can be found by a straightforward searching method. In addition to the abovementioned combined analysis method, the authors of [7] have also proposed an equal-incremental-fuel-cost method for the optimal dispatch of CHP plants, as well as the power and heating systems. However, this method cannot handle inequality constraints. In [17], an optimal dispatch method was proposed, which can utilize the heating network (pipes) as a heat storage system. Unlike a system with a single CHP plant (single source), a multiple-heat-source system can have different possible flow directions in some pipes. This characteristic can cause severe difficulties in modeling. Unfortunately, it was not considered in either [7] or [17]. In paper [18], the model included heat plants, heat storages and heating networks. However, the change in flow direction was also not considered. The model proposed in [19] considered a constant hydraulic process (constant mass flow rates and directions) but variable temperatures. Thus, the entire model becomes linear and easy to solve. However, this kind of model allows only limited flexibility from the dispatch of a multiple-heat-source system, because the temperature is varying in only a small range, which is much smaller than the range of varying flows. A flow can have flow rates from negative to positive, while temperature cannot go to zero or negative degrees. In addition, heat storage, which requires both positive (charge) and negative (discharge) power to be modeled, cannot dispatch in both modes by changing the temperature only. For this reason, varying flow rates and directions are very important and need to be modeled in an MES [20].

This paper will try to fill the gap left by the abovementioned methods. The main contributions of this paper are summarized as follows: 1) Varying mass flow rates and flow directions of district heating systems are modeled with analytical forms. This is further included in an optimization model so that the optimal mass flow profile of the heating network can be determined. 2) A heat-electricity-network constrained economic dispatch (ED) method is proposed, which is based on mixed integer conic programming (MICP) that can be efficiently solved by many commercial solvers. This ED model can be used to optimally dispatch a large portfolio of energy sources/storages of different types with respect to the network constraints. To our best knowledge, these two contributions did not appear in any previous work.

The rest of the paper is organized as follows. The proposed methodology is presented in Section 2 and Section 3, where Section 2 focuses on the modeling of energy networks through nonlinear models while Section 3 focuses on establishing an MICP model by the approximation and convexification of nonlinear constraints. In Section 4, case studies are presented and discussed. Conclusions are drawn in Section 5.

2. Modelling of an Integrated Heat-electricity Network

In this section, an integrated heat-electricity network will be modeled through general nonlinear models, which will be a starting point for the MICP based modeling presented in Section 3.

2.1 Notation of a Heat Network

To help understand the modeling in this paper, a few important notations will be introduced in this subsection. The pipe structure of a heat network is shown in Fig. 1. Variables ρ, x, m represent the pressure of a node, the mass flow rate of a pipe and the mass flow rate of a node, respectively. For brevity, variables in this paper are often used in a vector form. For example, a vector form variable, "ρ", can represent the pressure of all nodes, which is obtained by stacking the scalar variables into one column.

For brevity, the mass flow (x) of a pipe is addressed as a "line flow" and the mass flow (m) of sources, storages or loads as a "nodal flow". A nodal flow flows between the supply and return network through heat exchangers at load nodes or through heat plants at source nodes. Because of symmetry, the hydraulic process of the return network is not modeled. As shown in Fig. 1 (b) and (d), each line flow or nodal flow has an inlet temperature (T_s, u^+ or v^+) and an outlet temperature (T_r, u^- or v^-), and an absolute temperature drop ($\triangle T$, $\triangle u$ or $\triangle v$). Each node is associated with an auxiliary variable (T_{sm} or T_{rm}), which represents the temperature achieved after the mixing of the inflows. For brevity, it is addressed as a "mixed temperature".

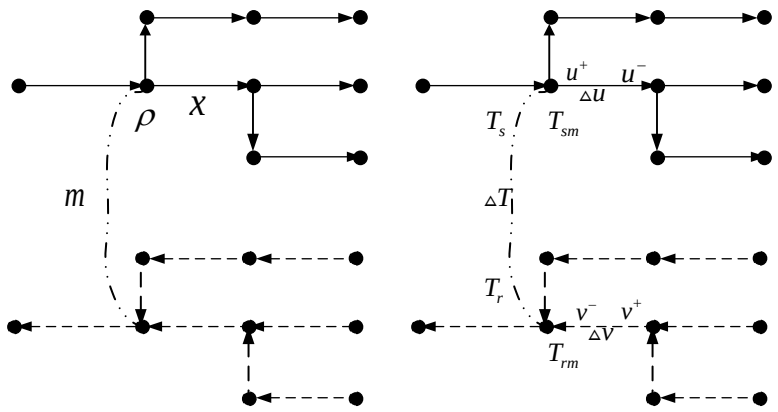

Fig. 1. (a) (b) represent respectively the hydraulic and thermal processes of a supply network; (c) (d) represent respectively the hydraulic and thermal processes of the return network

It is worthwhile to explain the incidence matrix of a network, denoted by A. A network is represented by a directed graph as shown in Fig. 1. A has elements either 1, -1 or 0. If $\{A\}_{i,j}$ (the element of the i-th row and the j-th column) is -1, then the j-th pipe's direction is pointing to the i-th node. If it is 1, the pipe's direction is opposite. Zero means no connection between the pipe and the node. Matrix A^+ is a partial matrix of A, which keeps all the '1' elements but let others be zero. Similarly, matrix A^- is a partial matrix of A, which keeps '-1' only. There is $A = A^+ + A^-$. Because a return network is symmetric to its supply network with a reversed direction (see Fig. 1), its incidence matrix is $-A$.

2.2 The Hydraulic and Thermal Processes of a Heat Network

There are two processes, i.e., hydraulic and thermal processes, that define a heat network model. The two

processes are coupled and influence each other, leading to the highly nonlinear model of a heat network. The hydraulic process is about the mechanics of the fluid, usually the hot water flowing in the pipes. The thermal process is about the temperature and heat exchange.

According to the fluid continuity, there is the mass flow rate relation at a given time t,

$$-Ax_t + m_t = 0, \forall t \in N_t \quad . \tag{1}$$

If a line flow, x_t, has (element-wisely; the same meaning when addressing vector variables in the rest of this paper) a positive value, the actual flow direction is along the predefined graph direction of the network; if x_t is negative, it flows in an opposite direction. A nodal flow, m_t, is positive (element-wisely) if it is an injection (source); it is negative if it is a load. For brevity, equations and inequalities are as often as possible in matrix forms in this paper, such as (1).

The pressure drop κ_t of pipes is calculated by,

$$\kappa_t = K * x_t * x_t, \forall t \in N_t . \tag{2}$$

Vector K is the hydraulic resistance coefficient, varying from pipe to pipe. The pressure drop is proportional to the square of the mass flow rate. Here, '*' means element-wise multiplication. Equations (1)-(2) define a hydraulic process. The maximum total pressure drop along the pipes in a network is limited by the maximum capacity of the pumps. To model the pressure at each node, an auxiliary binary variable is needed, which indicates the real flow directions and is denoted by y. If y is 1, the real flow direction agrees with the predefined graph direction, which also means $x \geq 0$; otherwise, the real flow direction is opposite to the predefined one, which means $x \leq 0$. Assume that the nodal pressure levels (of a supply network) are ρ_t, there are:

$$A^T \rho_t \geq \kappa_t + M(y_t - 1), \forall t \in N_t , \tag{3}$$

$$-A^T \rho_t \geq \kappa_t - My_t, \forall t \in N_t . \tag{4}$$

In (3)-(4), M is a big number. The result of using M is: $A^T \rho_t \geq \kappa_t$ is valid only if y is 1, and $-A^T \rho_t \geq \kappa_t$ is valid only if y is 0. By using this method, the relation between the pressure level of each node and the pressure drop of each pipe is correctly established according to the actual flow direction y.

The pressure level should be within a limit:

$$\rho^{MIN} \leq \rho_t \leq \rho^{MAX} \tag{5}$$

In addition, y should agree with the sign of x :

$$-M(1 - y_t) \leq x_t \leq My_t, \ \forall t \in N_t \tag{6}$$

For a thermal process, the relation among the nodal flow m, the nodal temperature loss $\triangle T$ and the thermal power Φ is expressed as,

$$\Phi_t = c_p(\triangle T_t * m_t), \forall t \in N_t , \tag{7}$$

$$\triangle T_t = T_{s,t} - T_{r,t}, \forall t \in N_t . \tag{8}$$

c_p is the heat capacity of the fluid. Equations (7) and (8) represent all types of nodes, including loads, sources and storages. The nodal temperature loss ($\triangle T_t$) is defined as the temperature difference between the supply and return networks at each node. It should be noted that the temperature of a supply network is always higher than the return network.

The line flow temperature drop $\triangle u_t$ of a supply network is calculated by,

$$\left(u_t^+ - T_{a,t}\right) = \left(u_t^- - T_{a,t}\right) * e^{-\frac{\lambda L}{c_p x_t}}, \forall t \in N_t \quad , \tag{9}$$

$$\triangle u_t = \left|u_t^+ - u_t^-\right|, \forall t \in N_t , \tag{10}$$

where $T_{a,t}$ is the time-varying ambient temperature, λ is the heat transfer coefficient and L is the length of the pipes.

Similarly, for a return network, the temperature drop Δv_t is,

$$\left(v_t^+ - T_{a,t}\right) = \left(v_t^- - T_{a,t}\right) * e^{-\frac{\lambda L}{c_p x_t}}, \forall t \in N_t, \tag{11}$$

$$\Delta v_t = \left|v_t^+ - v_t^-\right|, \ \forall t \in N_t. \tag{12}$$

For a supply network, the model of the flow and temperature mixing at each node is expressed as,

$$-A^+(x_t * u_t^+) - A^-(x_t * u_t^-) + m_t * T_{s,t} = 0, \forall t \in N_t; \tag{13}$$

For a return network, the model is,

$$A^-(x_t * v_t^+) + A^+(x_t * v_t^-) - m_t * T_{r,t} = 0, \forall t \in N_t. \tag{14}$$

In addition, it is required that the temperature of all outflows at each node should be the same as the mixed temperature (assuming that the inflows are sufficiently mixed at each node), denoted by $T_{sm,t}$ and $T_{rm,t}$. This poses severe difficulties to the modeling which has not been properly modeled by any previous work. Here, by using the binary variable y and the big number M, it can be modeled as,

$$T_{sm,t} - M(1-y_t) \le A^+ u_t^+ \le T_{sm,t} + M(1-y_t), \forall t \in N_t, \tag{15}$$

$$T_{sm,t} - My_t \le -A^- u_t^- \le T_{sm,t} + My_t, \forall t \in N_t, \tag{16}$$

$$T_{rm,t} - M(1-y_t) \le -A^- v_t^+ \le T_{rm,t} + M(1-y_t), \forall t \in N_t, \tag{17}$$

$$T_{rm,t} - My_t \le A^+ v_t^- \le T_{rm,t} + My_t, \forall t \in N_t. \tag{18}$$

Inequalities (15)-(16) can make sure that the mixed temperature $T_{sm,t}$ equals the temperature of all "real" outflows (not just according to the predefined graph directions). Similarly, (17)-(18) do the same tasks for the return network.

It is assumed that the supply temperatures $T_{s,t}$ of source nodes are given, such as 80 °C. If a source node is turned into a load node, e.g. a storage can be both charging or discharging, this requirement is not enforced. Instead, the requirement of a load node is enforced. For load nodes, the supply temperature should equal to the mixed temperature since the nodal flow is an outflow from the node:

$$T_{s,t} = T_{sm,t}. \tag{19}$$

And for source nodes, the return temperature should equal to the mixed temperature since it is an outflow:

$$T_{r,t} = T_{rm,t}. \tag{20}$$

The mixed temperature at the nodes of a supply network has limits:

$$T_s^{MIN} \le T_{sm,t} \le T_s^{MAX}. \tag{21}$$

The mixed temperature limit of a return network is not enforced, as it is expected that the return network has a lower temperature loss due to its lower temperature level than the supply network. If (21) is satisfied, the mixed temperature of the return network should have no issues as well.

2.3 Sources

In this paper, a CHP is considered as a representative co-generation source, which connects the heat and electricity network. For CHPs,

$$\phi_{g,t} = \pi p_{g,t}, \forall t \in N_t, \tag{22}$$

$$p_g^{\min} \le p_{g,t} \le p_g^{\max}, \forall t \in N_t. \tag{23}$$

π is the heat to power ratio of a CHP, $p_{g,t}$ and $\phi_{g,t}$ are the electric and thermal power, respectively. An electric boiler or heat pump can also be modeled through (22)-(23). The difference is that for a CHP, $\pi \ge 1$ (e.g., 1.3), while for a boiler or heat pump, $\pi \le 0$ (e.g., -1 or -2.3). This means that a boiler or heat pump will consume electric power in order to produce heat.

Heat accumulators (HA) have been considered in this paper in order to harvest some extra flexibility from a MES. They are modeled as,

$$\theta_0 - \sum_{t'<=t} \phi_{c,t'} = \theta_t, \forall t \in N_t, \tag{24}$$

$$-\phi_c^{MAM} \le \phi_{c,t} \le \phi_c^{MAX}, \tag{25}$$

$$\theta^{MIN} \le \theta_t \le \theta^{MAX}, \forall t \in N_t. \tag{26}$$

θ_0 and θ_t are the heat energy levels of an HA, while $\phi_{c,t}$ is the charging or discharging power of the HA. ϕ_c^{MAX} is the maximum power of the HA. θ^{MIN} and θ^{MAX} are the minimum and maximum energy level of the HA.

In addition, waste heat from industrial activities is also included, which can contribute to a MES with very cheap heat energy. A waste heat ($\phi_{w,t}$) source is modeled as a negative heat load with possible curtailments:

$$0 \le \phi_{w,t} \le \phi_w^{MAX}, \forall t \in N_t. \tag{27}$$

The nodal thermal power is determined by,

$$\Phi_t = B_g \phi_{g,t} + B_c \phi_{c,t} + B_w \phi_{w,t} + B_d \phi_{d,t} \tag{28}$$

where B is the corresponding heat-source-to-node incidence matrix. Similarly, one can model renewable electricity sources and storages, such as photovoltaic systems (PV) by,

$$0 \le p_{pv,t} \le p_{pv}^{MAX}, \forall t \in N_t. \tag{29}$$

And batteries,

$$\theta'_0 - \sum_{t'<=t} p_{b,t'} = \theta'_t, \forall t \in N_t, \tag{30}$$

$$-p_b^{MAX} \le p_{b,t} \le p_b^{MAX}, \tag{31}$$

$$\theta'^{MIN} \le \theta'_t \le \theta'^{MAX}, \forall t \in N_t, \tag{32}$$

where $p_{pv,t}$ and $p_{b,t}$ are the power of PVs and batteries, θ'_0 and θ'_t are the state of charge (SOC) levels of the batteries.

2.4 Electrical Distribution Networks

The reference bus of an electrical network is the bus connected with the external grid. Assume that the system imported (or exported) power from the external grid is p_0. For simplification, a linear DC model is employed to model the power balance and the line flows (P) in this study:

$$p_{0,t} + sum\{p_{g,t}\} + sum\{p_{d,t}\} + sum\{p_{b,t}\} + sum\{p_{pv,t}\} = 0, \forall t \in N_t, \tag{33}$$

$$P_t = D_g p_{g,t} + D_d p_{d,t} + D_{pv} p_{pv,t} + D_b p_{b,t}, \forall t \in N_t, \tag{34}$$

$$p_0^{\min} \le p_{0,t} \le p_0^{\max}, \forall t \in N_t, \tag{35}$$

$$-P^{\max} \le P_t \le P^{\max}, \forall t \in N_t. \tag{36}$$

$sum\{\}$ means the sum of the elements of a vector. $p_{d,t}$ is the power of loads. Constraint (33) states that the total power is balanced. Constraint (34) relates the line flows P to nodal generations and loads via the power transfer distribution factor D_g and D_d, etc. (35)-(36) represent the limitations of the imported/exported power and the line flows.

An ED problem is to minimize the total energy cost over the defined periods with respect to the demands and the network constraints. In the above analysis, many network constraints, especially the heat network constraints, are highly nonlinear and nonconvex; therefore, if simplification is not exercised, the ED model will end up with a general nonlinear model. In general, a nonlinear and nonconvex model is intractable. Hence, in Section 3, simplification and convexification will be employed to formulate a tractable ED model.

3. Economic Dispatch Model through Mixed Integer Conic Programming

In this section, the ED model of a MES will be formed through MICP, which can be solved by many powerful commercial solvers, such as CPLEX. The task is done by reforming the nonlinear constraints in Section 2 to linear and/or conic constraints.

In this paper, the ED is used for day-ahead energy planning, which plans the energy sources (CHP, HA, the bulk grid, industrial waste heat, etc.) of a MES for the next day (24 hours).

The objective is to minimize the total energy cost, which consists of the cost of importing electricity from the bulk grid and the costs of local heat/power sources, such as CHPs and waste heat [21].

$$\min \sum_{t \in N_t} (c_t p_{0,t} + b_g{}^T p_{g,t} + b_w{}^T \phi_{w,t} + b_{pv}{}^T p_{pv,t}), \tag{37}$$

where c_t, b_g, b_w, b_{pv} are the prices of the power exchanged with the bulk grid, CHPs, waste heat and PV, respectively. The objective function (37) is subject to the following reformed linear and/or conic constraints.

3.1 The Hydraulic Constraints of a Heat Network

The constraint (1) is already a linear one, which is acceptable to any MICP solver. The pressure loss constraint, (2), is nonconvex and can be convexified to a conic constraint as,

$$K * x_t * x_t \le \kappa_t, \forall t \in N_t . \tag{38}$$

Such convex relaxation will not affect the optimization results, since the goal is to limit the maximal pressure loss.

In summary, the hydraulic constraints are: (1), (3)-(6), (38).

3.2 The Thermal Constraints of a Heat Network

For the convenience of calculation, one of the nodes is chosen to be the reference node, which is responsible for the thermal power balance of the whole network: the total heat supply equals the total heat demand plus the total heat losses. Nowadays, many heat networks have only one heat source, which will naturally be the reference node. In the future, as the concepts of smart energy grids and MES gain more and more attention and practices, the heating network is required to integrate more heat sources, e.g., heat sources provided by industrial customers (waste heat) and/or small distributed CHPs.

In order to integrate multiple heat sources into a system, it is beneficial to have a roughly fixed temperature profile, but variable mass flow rates of the system, as was discussed in Section 1 (Introduction). The temperature optimization can be done separately, which is to choose an optimal supply temperature level for the system. In this paper, the optimal supply temperature is given as an input to the ED model, which could be, e.g., 100, 80 or 60 °C. Each source node has a given supply temperature.

3.2.1 Heating power and its balance:

In order to avoid inconsistency, there are different rules about (7)-(8) depending on the node type. For the reference node, if it is a source, (7)-(8) are not enforced; if it is a load, only (8) is enforced. For other nodes, if they are load nodes, (7)-(8) are enforced and ΔT_t is given as a parameter, such as 30 °C. If they are source nodes, only (7) is enforced with a given ΔT_t, which could be 31~33 °C depending on the insulation level of the whole network. Consequently, (7)-(8) are linearized for all types of nodes. Moreover, the power of each nonreference node can be calculated by (7) with the given ΔT_t.

A supply network has a temperature level close to the given supply temperature (e.g. 80 °C), denoted by T_s^{ref}, everywhere and the return network has a temperature level close to T_r^{ref} (e.g. 50 °C) everywhere. The losses ($\varepsilon_{s,t}$ and $\varepsilon_{r,t}$) depend on the temperature level of mass flows, the ambient temperature (T_a) and the insulation of the pipes (λ). Therefore, the loss of each pipe of the supply network can be estimated by,

$$\varepsilon_{s,t} = (u_t^+ - T_a) * \lambda * L \approx (T_s^{ref} - T_a) * \lambda * L = \overline{\varepsilon}_{s,t} . \tag{39}$$

And the loss of each pipe of the return network,

$$\varepsilon_{r,t} = (v_t^+ - T_a) * \lambda * L \approx (T_r^{ref} - T_a) * \lambda * L = \overline{\varepsilon}_{r,t} . \tag{40}$$

Since the losses are constant, we use $\overline{\varepsilon}_{s,t}$ and $\overline{\varepsilon}_{r,t}$ instead of $\varepsilon_{s,t}$ and $\varepsilon_{r,t}$. Then, the heat power of the reference node can be determined by the overall power balance, i.e.:

$$sum\{\phi_{g,t}\} + sum\{\phi_{c,t}\} + sum\{\phi_{w,t}\} + sum\{\phi_{d,t}\} + sum\{\overline{\varepsilon}_{s,t}\} + sum\{\overline{\varepsilon}_{r,t}\} = 0 . \tag{41}$$

3.2.2 The temperature drop along pipes:

Employing the approximating method, $e^t \approx 1 + t$ for small t, one can simplify the temperature loss constraints (9)-(12) to,

$$\begin{aligned} &\left(u_t^- - T_{a,t}\right) \approx \left(u_t^+ - T_{a,t}\right) * (1 - \frac{\lambda * L}{c_p x_t}), \forall t \in N_t \\ &\Rightarrow c_p (u_t^+ - u_t^-) * x_t = \lambda * L * \left(u_t^+ - T_{a,t}\right), \forall t \in N_t \quad , \\ &\Rightarrow c_p \Delta u_t * X_t = \varepsilon_{s,t}, \forall t \in N_t \end{aligned} \tag{42}$$

and

$$c_p \Delta v_t * X_t = \varepsilon_{r,t}, \forall t \in N_t . \tag{43}$$

where $X_t = |x_t|$ is the absolute value of the mass flow rate. We assume that the heat network is well insulated, and the temperature drops are small; therefore, the above approximation is reasonable. But they are still nonconvex. By relaxing "=" to "$\geq$ " and approximating the right-hand side terms to constants $\overline{\varepsilon}_{s,t}$ and $\overline{\varepsilon}_{r,t}$, one can obtain the following conic constraints:

$$c_p \Delta u_t * X_t \geq \overline{\varepsilon}_{s,t}, \forall t \in N_t , \tag{44}$$

$$c_p \Delta v_t * X_t \geq \overline{\varepsilon}_{r,t}, \forall t \in N_t , \tag{45}$$

and linear constraints ensuring the relation between X_t and x_t:

$$X_t \leq x_t + (1 - y)M , \tag{46}$$

$$X_t \leq -x_t + yM , \tag{47}$$

where $\Delta u_t \geq 0, \Delta v_t \geq 0, X_t \geq 0$. This relaxation will not affect the optimization results, because X_t is bounded and $\Delta u_t, \Delta v_t$ are to be minimized. The approximating of the right-hand side of (44)-(45)is reasonable since it is assumed that the temperature drops are marginal. It should be noted that the convex relaxation ((44)-(45)) of (9)-(12) is much more accurate than the simple linearization of (9)-(12), because these conic constraints can well catch the fact that the temperature drop is reversely proportional to the mass flow rate X_t. This is especially critical when X_t is varying in the large range from zero to the peak. It should be pointed out that when the mass flow rate of a pipe is small, the temperature drop will be large (reverse proportional). But this large temperature drop will not affect the mixed temperature at the subsequent nodes since the mass flow rate of it is small. Therefore, it is still valid to assume that the temperature drop of the overall network is small.

3.2.3 Mixed temperature of inlet flows:

Convexifying the temperature/flow mixing constraints of (13)-(14) is even more challenging. Here, the mixed temperature is approximated to the temperature of the largest inflow of each node, since this flow is dominating the flow mixing result. As a line flow or a nodal flow can only be dominating at most once for a supply network and at most once for the return network as well, we introduce new auxiliary binary-variables as follows. Binary vector variables z^+_t (for the inlet ends of pipes) and z^-_t (for the outlet ends of pipes) indicate whether the line flow in a supply network is dominating (=1 means dominating). Similarly, vector

variables $z^{+}{}'_{t}, z^{-}{}'_{t}$ and $z_{0,t}$ indicate whether each line flow of the return network and each nodal flow are dominant, respectively. Also, μ_t, μ'_t are introduced representing the corresponding maximum inflow of each node of the supply network and the return network, respectively. Then, there are the following constraints for a supply network.

$$-A * x_t^T \le \mu_t, \forall t \in N_t \tag{48}$$

$$m_t \le \mu_t, \forall t \in N_t \tag{49}$$

$$-A * x_t^T + (1 - A^+ * z^+{}_t^T + A^- * z^-{}_t^T)M \ge \mu_t, \forall t \in N_t \tag{50}$$

$$m_t \ge (z_{0,t} - 1)M + \mu_t, \forall t \in N_t \tag{51}$$

$$A^+ z^+{}_t - A^- z^-{}_t + z_{0,t} = 1 \tag{52}$$

$$z^+{}_t \le 1 - y_t \tag{53}$$

$$z^-{}_t \le y_t \tag{54}$$

$$\Delta u_t + (z^-{}_t + y_t - 2)M \le A^T T_{sm,t} \le \Delta u_t + (2 - z^-{}_t - y_t)M \tag{55}$$

$$-\Delta u_t + (z^+{}_t - y_t - 1)M \le A^T T_{sm,t} \le -\Delta u_t + (1 - z^+{}_t + y_t)M \tag{56}$$

$$T_{s,t} + (z_{0,t} - 1)M \le T_{sm,t} \le T_{s,t} + (1 - z_{0,t})M \tag{57}$$

Constraints (48)-(49) ensure that the maximum inflow μ_t of each node is larger than all its inflows. The element-wise multiplying '*' of a matrix A and a row vector x_t^T is done like this: each row of A multiplies x_t^T (element-wise). The resulting matrix has the same size of A. As usual, $\le$ in (48) is element-wise comparative. Constraints (50)-(51) assure that the selected maximum inflow of each node is no less than μ_t. Therefore, (48)-(51) together can make sure that μ_t is the maximum inflow. Constraint (52) states that each node has exactly one selected maximum flow, and (53)-(54) state that only one of $z^+{}_t$, $z^-{}_t$ can be selected, depending on y_t. Constraints (55)-(56) state that if a line flow is selected, the temperature drop along this line flow (pipe) must be equal to the difference of the mixed temperature of its two terminal nodes. Constraint (57) states that if a nodal flow is selected, the mixed temperature must be equal to the nodal flow temperature.

Similarly, for the return network, there are constraints:

$$A * x_t^T \le \mu'_t, \forall t \in N_t \tag{58}$$

$$-m_t \le \mu'_t, \forall t \in N_t \tag{59}$$

$$A * x_t^T + |A| * (1 - z^{+}{}'^{T}_{t} - z^{-}{}'^{T}_{t})M \ge \mu'_t, \forall t \in N_t \tag{60}$$

$$-m_t \ge (z'_{0,t} - 1)M + \mu'_t, \forall t \in N_t \tag{61}$$

$$-A^- z^{+}{}'_t + A^+ z^{-}{}'_t + z'_{0,t} = 1 \tag{62}$$

$$\Delta v_t + (z^{+}{}'_t + z^{-}{}'_t + y_t - 2)M \le -A^T T_{rm,t} \le \Delta v_t + (2 - z^{+}{}'_t - z^{-}{}'_t - y_t)M \tag{63}$$

$$-\Delta v_t + (z^{+}{}'_t + z^{-}{}'_t - y_t - 1)M \le -A^T T_{rm,t} \le -\Delta v_t + (1 - z^{+}{}'_t - z^{-}{}'_t + y_t)M \tag{64}$$

$$T_{r,t} + (z'_{0,t} - 1)M \le T_{rm,t} \le T_{r,t} + (1 - z'_{0,t})M \tag{65}$$

In summary, the thermal constraints for pipes are: (39)-(41), (44)-(47), and for nodes are: (7)-(8), (19)-(21), (48)-(65).

Finally, one can combine the source constraints and power system constraints from Section 2 to achieve the final ED problem, which is: (37), subject to the hydraulic constraints (1), (3)-(6), (38), the thermal constraints for pipes (39)-(41), (44)-(47), the thermal constraints for nodes (7)-(8), (19)-(21), (48)-(65), and constraints (22)-(36).

4. Case Studies

A representative heat-electricity system is employed in the case study, which can supply energy to a local area. The structure of this system is shown in Fig. 2. A CHP unit and a waste heat source (from an industrial process) supply the district heating network, while the external grid, the CHP and a PV plant together power up the electricity network. The CHP is equipped with a HA, while the PV plant is equipped with a battery system. The district heating network consists of 4 pipelines and 5 nodes for the supply network and the same number of pipes and nodes for the return network (for brevity, not shown in the figure). Node 1 is coupled with the electricity bus, Bus 1, through the CHP unit. Buses 2, 3, 4 and Nodes 2, 3, 5 are electricity load buses and heat load nodes, respectively. Each load node or bus is a substation and can supply tens of end users (not shown).

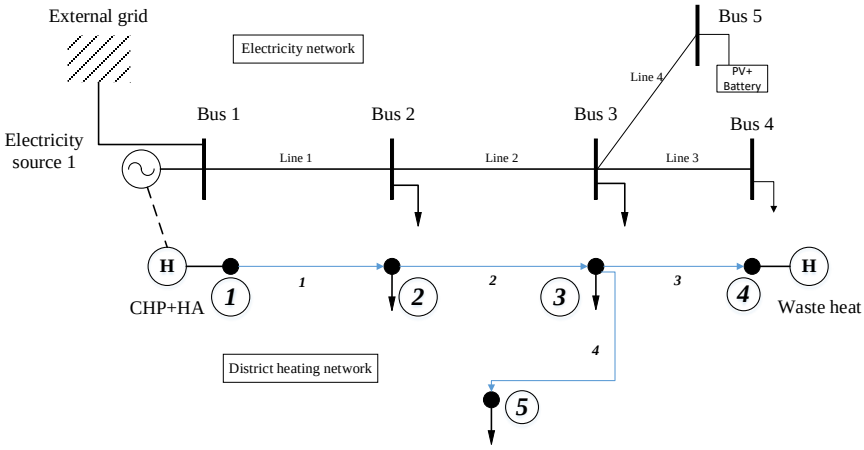

Fig. 2. Single line diagram of the electricity distribution network and the district heating network

The key parameters of the integrated electricity-heating system are listed in Table I. The pipes have the same length, as well as the heat transfer coefficient, but different hydraulic resistances. Bus 1 and Node 1 are the reference bus and node respectively. Both the heat and electric loads are time-varying, and their peaks are listed in Table I.

Because of HA, Node 1 can be both a source node or a load node depending on the operation mode. As discussed at the end of Section 3, when it is a source node, it has a supply temperature of 80 °C; when it is a load node, it has the temperature drop of 30 °C. The ambient temperature and the prices are shown in Fig. 3 and Fig. 4 respectively. The waste heat has a very low price. PV has a zero price; therefore, it is not shown in these figures.

It should be noted that the proposed model is flexible in terms of the time resolution of the planning. It is possible to have different time resolutions of the scheduling for heat and electricity systems. The reason is that the time constant (response time) of the heat sector is much slower than the power sector. In this case study, there are 6 4-hour periods for the heating system while there are 24 1-hour periods for the electricity system. But they both have the same total length: 24 hours.

TABLE I
KEY PARAMETERS OF THE SIMULATION MODEL

parameter	value
Heat capacity of mass flow c_p (MJ/kg/K)	$4.812\text{x}10^{-3}$
Length of each pipe L (m)	400
Hydraulic resistance K of pipe 1 (1/kg/m)	0.0379
Hydraulic resistance K of pipe 2/3/4	0.1379
Heat transfer coeff. λ (MW/m/K)	$0.2\text{x}10^{-6}$
Peak Heat load at node 2, 3, 5 (MW)	-0.3
Peak power of the waste heat (MW)	1
Maximum power of the HA (MW)	±1
Initial and maximum capacity of HA (MWh)	0.5 / 2
Supply temperature at source nodes (ºC)	80
Temperature drop at load node (ºC)	30
Heat / power ratio for CHP	1.3
Peak load at bus 2, 3,4 (MW)	-0.15
Maximum PV power (MW)	0.5
Maximum CHP power (electricity) (MW)	2
Maximum power of battery (MW)	+/-0.4
Initial and maximum SOC of battery (MWh)	0.4 / 0.8
Pressure limit (MPa) HIGH/LOW	11/4
Line flow limit (MW)	0.6
Minimum supply temperature at load nodes (ºC)	75

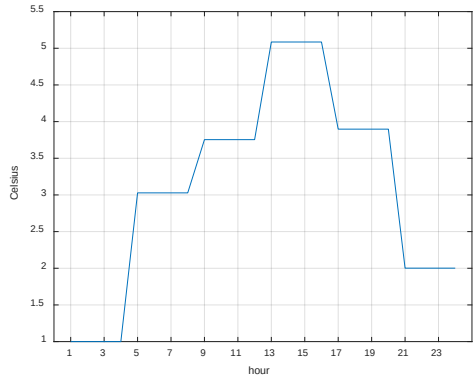

Fig. 3. The ambient temperature profile

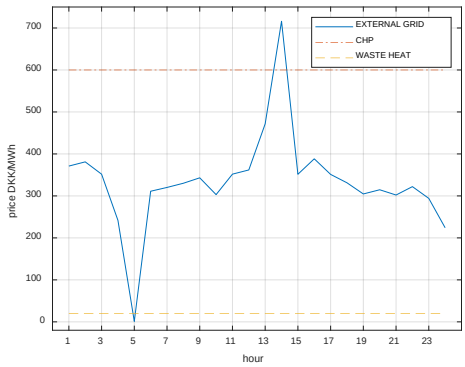

Fig. 4. The price of different sources

4.1 Case Study Results

In the case study, the MICP based ED model was programmed with Matlab + YALMIP [22], and the MICP solver was CPLEX [23]. It should be noted that, in YALMIP, the command “cone” or “rcone” should be used for programming the conic or rotated conic constraints. The model has around 90 discrete variables, 800 continuous variables and 1600 constraints, including 90 conic constraints. One simulation can be completed in 0.2 second on a laptop with an INTEL i7 CPU.

Three scenarios were studied. In the first scenario, optimization was not employed. The battery, as well as the HA, was not used. The PV and the waste heat were used to supply the loads; if not sufficient, the CHP, as well as the bulk grid, will be utilized. In the second scenario, optimization was employed, as well as the battery and HA. However, the network constraints were not considered. In the third scenario, the full ED model was considered. The costs of the three scenarios are shown in Table II, which are the prices to buy the required energy, including the imported/exported power. The difference of with or without optimization is significant.

The details are discussed in the following.

TABLE II
SCENARIOS AND COSTS COMPARISON

	Scenario One:	**Scenario Two:**	**Scenario Three**
Optimization	No	Yes	Yes
HA and Battery (electric)	No	Yes	Yes
Network constraints	No	No	Yes
Total cost (DKK)	4663.5	2611.4	2826.2

For the first scenario, the scheduling results are shown in Fig. 5. The first subgraph shows the pressure profiles of Node 1 and 4. It can be seen that Node 4 has an over pressure during the time 17~20h (=17:00~20:59). Because in this period, the entire heat system is supplied by the waste heat as shown in the second subgraph. The waste heat can supply the entire heat system during the time 9~20h. The CHP plant supplies the system in the rest of the day. Because the hydraulic resistance of Pipe 1 is much lower than the other pipes, the CHP can supply the whole system without pressure problems. The total heat load in the daytime is slightly lower than at night. During the time 17~20h, the entire electric system is supplied by the external grid because the CHP does not run, and the PV power is too low. The system exports electricity when the PV power is high during 10~14h and when the CHP runs during 1~8h and 21~24h.

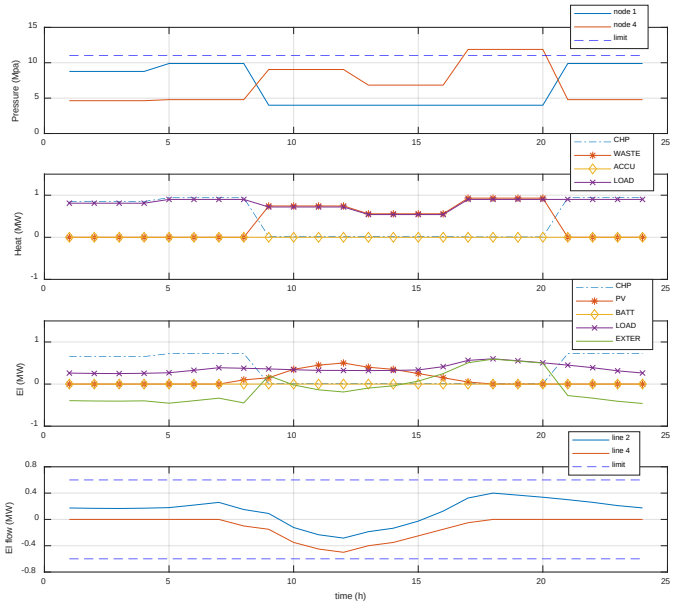

Fig. 5. Scheduling results for the first scenario: no optimization, no storage

The scheduling results of the second scenario are shown in Fig. 6. The integrated heat and electricity system are optimized. The cost is largely reduced compared to the first scenario; however, the network limits are violated in several periods. Because of the HA, the waste heat is able to run at its full power (1MW) throughout 9~20h (the industrial process is shut down during the rest of the day). Furthermore, the CHP is running throughout 13~16h because of the high system price (excessive electricity is sold at this price). All excessive heat is stored in the HA and then discharged in peak periods: 5~9h and 21~24h. For the electricity system, the electricity is imported when the price is low and exported when the price is high.

In fact, both Scenario One and Two are infeasible in terms of the network limits. Hence in Scenario Three, the network's limits are included in the ED model. As shown in Fig. 7, both the pressure limits of the heating system and the line flow limits of the electric system are respected. Because of the pressure limits, the waste

heat is not running at its full power during the time 9~20h. Due to the line flow limits of Line 4, the battery discharging power is reduced during the time 13~14h. For a similar reason, the battery charging power is reduced in the periods 19h and 21h. Although the total energy cost is slightly increased compared to Scenario Two, the network limits are well respected. In all three scenarios, the first one is the worst: it not only has the highest cost, but also violates several network limits. This shows that the ED model proposed in this paper has a significant value for MES planning.

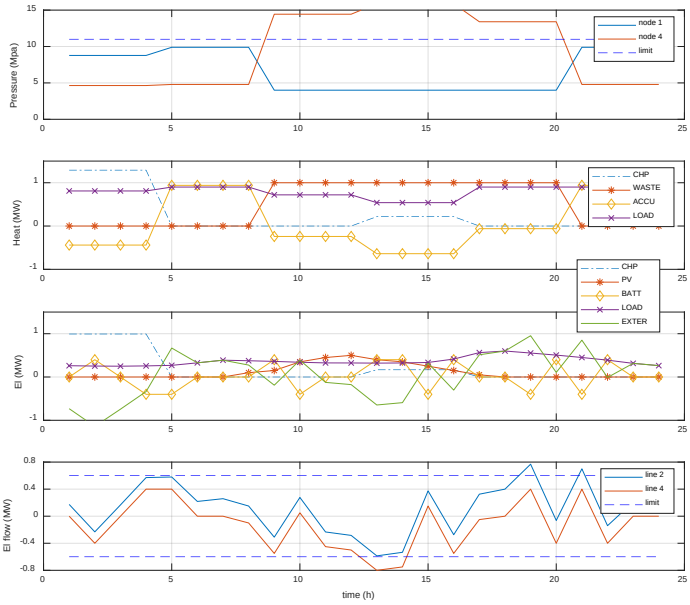

Fig. 6. Results of scenario 2: optimization without network constraints

Lastly, we checked the optimal mass flow profiles and the thermal (temperature) profiles of the heating system for Scenario Two and Three during the critical period: 17~20h. The results are shown in Fig. 8 and Fig. 9. The numbers below a pipe are mass flow rates and the temperature drop along the pipe. The numbers associated with a node are the mixed temperature, the nodal flow rate and the power of the node. For Scenario Two, the waste heat runs at its full power 1 MW, and the HA charges at 0.06 MW, both of which can be seen from the mass flow rates/directions shown in Fig. 8. For example, -0.51 kg/s (-0.06 MW) at Node 1 indicates that the HA is in a charging state (functioning as a heat load), while 7.68 kg/s (1 MW) at Node 4 indicates that the waste heat is supplying heat power. The supply temperature at Node 1 is 76.68 ºC, not 80 ºC, because the HA is charging, and the node is a load node. It can be seen that all the mixed temperature (T_{sm}) of the supply network is within the allowed range 75~80 ºC. The total thermal loss is about $1-0.03*3-0.06=0.04$ MW.

Similarly, the hydraulic and thermal profiles of Scenario Three are shown in Fig. 9. As discussed before, the waste heat is not in its full power because of the pressure limit. The HA is discharging (0.06 MW, 0.48 kg/s) in order to balance the heat demand and losses. Now, the supply temperature at Node 1 is 80 ºC as expected.

Meanwhile, it can be seen that both the mass flow rates and directions change according to the optimal dispatch results of the HA and waste heat. Comparing the two scenarios, the mass flow rate changes in pipe 1/2/3, while the flow direction changes in pipe 1 only.

It should be noted that the thermal profiles are re-calculated based on the power determined by the ED model of Scenario Two and Three, respectively. Because of the convex relaxation, the ED model itself is not able to produce a correct temperature profile — the model only ensures that the mixed temperature is within the range 75~80 ºC.

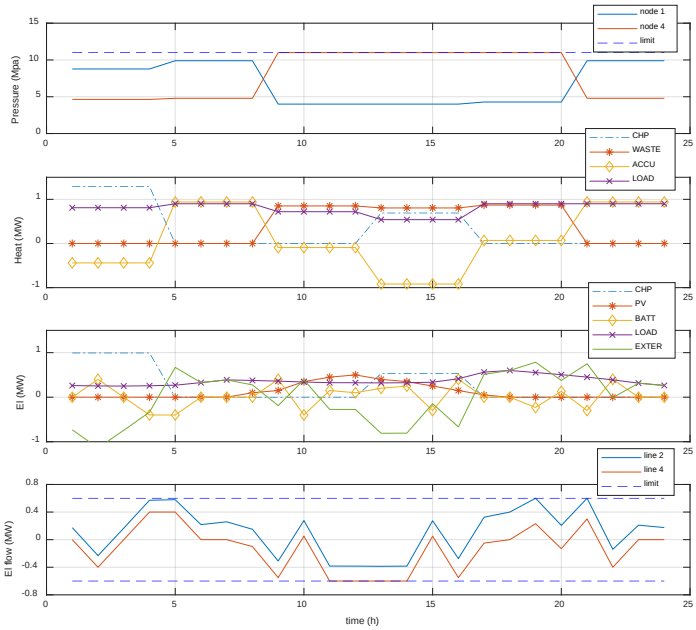

Fig. 7. Results of scenario three: optimization with network constraints

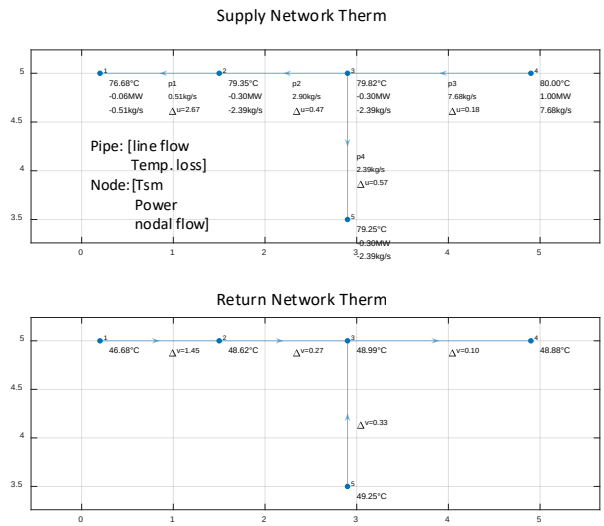

Fig. 8. Mass flow and thermal profile of Scenario Two at 17~20h

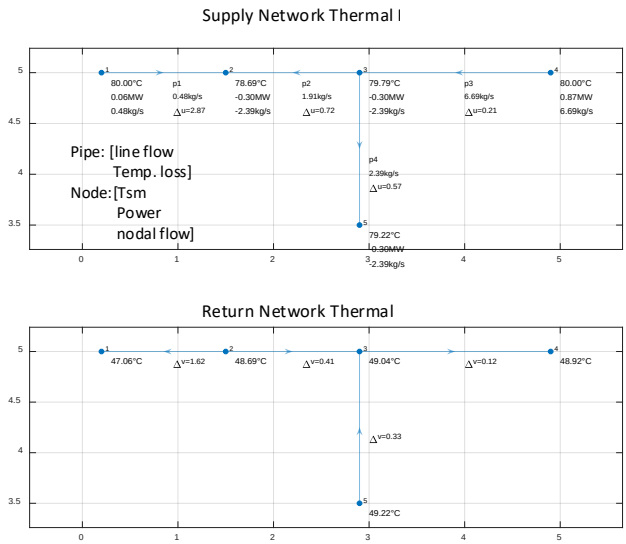

Fig. 9. Mass flow and thermal profile of Scenario Three at 17~20h

5. Conclusions

This paper has proposed an MICP based ED model for an MES, which can optimally dispatch a large portfolio of energy sources of different types, including the exchange power with the external grid. The model takes into account the network constraints of both sectors: heating and power. Moreover, both the thermal and hydraulic processes of the heating sector are modeled in this model. The proposed model can also determine the optimal mass flow (rates and directions) along with the optimal power dispatch results, which has not been studied in any previous work.

The case study results of three scenarios show that the proposed ED model is efficient in terms of both the computation time and the cost savings. The first scenario represents those methods proposed in previous papers, which do not employ optimization and storage; therefore, the cost could be high. The second scenario represents those methods which only consider the characteristics of energy sources (cost, output power, limits, etc.), but not the networks that deliver the energy to the end users. Therefore, the network limits may not be respected. The last scenario represents the method proposed in the current paper.

For the future work, it is interesting to investigate the accuracy of the proposed model when the temperature drop along a pipe is large (e.g., if the insulation is poor). The convexification and linearization method employed in the proposed model may lead to degraded accuracy. It is also interesting to propose new models if the accuracy of the current model is degraded.

References

[1] H. Lund, B. Möller, B. V. Mathiesen, and A. Dyrelund,“The role of district heating in future renewable energy systems,” *Energy*, vol.35, no.3, pp. 1381–1390, Mar. 2010.

[2] B. Rezaie and M. A. Rosen,“District heating and cooling: Review of technology and potential enhancements,” *Appl. Energy*, vol.93, pp. 2–10, May 2012.

[3] H. Lund, S. Werner, R. Wiltshire, S. Svendsen, J. E. Thorsen, F. Hvelplund, and B. V. Mathiesen,“4th

Generation District Heating (4GDH): Integrating smart thermal grids into future sustainable energy systems," *Energy*, vol.68, pp. 1–11, Apr. 2014.

[4] H. Cai, S. You, J. Wang, H. W. Bindner, and S. Klyapovskiy,"Technical assessment of electric heat boosters in low-temperature district heating based on combined heat and power analysis," *Energy*, vol.150, pp. 938–949, May 2018.

[5] Z. Pan, Q. Guo, and H. Sun,"Interactions of district electricity and heating systems considering time-scale characteristics based on quasi-steady multi-energy flow," *Appl. Energy*, vol.167, pp. 230–243, Apr. 2016.

[6] X. Liu and P. Mancarella,"Modelling, assessment and Sankey diagrams of integrated electricity-heat-gas networks in multi-vector district energy systems," *Appl. Energy*, vol.167, pp. 336–352, Apr. 2016.

[7] X. Liu, J. Wu, N. Jenkins, and A. Bagdanavicius,"Combined analysis of electricity and heat networks," *Appl. Energy*, vol.162, pp. 1238–1250, Jan. 2016.

[8] Jinni Dong, Q. Guo, H. Sun, and Z. Pan,"Research on state estimation for combined heat and power networks," in *Proc. 2016 IEEE Power and Energy Society General Meeting (PESGM)*, pp. 1–5.

[9] T. Sheng, Q. Guo, H. Sun, Z. Pan, and J. Zhang,"Two-stage State Estimation Approach for Combined Heat and Electric Networks Considering the Dynamic Property of Pipelines," *Energy Procedia*, vol.142, pp. 3014–3019, Dec. 2017.

[10] G. Gambino, F. Verrilli, M. Canelli, A. Russo, M. Himanka, M. Sasso, S. Srinivasan, C. Del Vecchio, and L. Glielmo,"Optimal operation of a district heating power plant with thermal energy storage," in *Proc. 2016 American Control Conference (ACC)*, pp. 2334–2339.

[11] X. Chen, C. Kang, M. O 'malley, Q. Xia, J. Bai, C. Liu, R. Sun, W. Wang, and H. Li,"Increasing the Flexibility of Combined Heat and Power for Wind Power Integration in China: Modeling and Implications," *IEEE Trans. POWER Syst.*, vol.30, no.4, 2015.

[12] F. Wu, S. Huang, R. Li, Q. Guo, H. Sun, and Z. Pan,"Research on the Collaborative Optimization of Multi-Energy Flow Microgrids," *Energy Procedia*, vol.103, pp. 345–350, Dec. 2016.

[13] I. Dimoulkas and M. Amelin,"Probabilistic day-ahead CHP operation scheduling," in *Proc. 2015 IEEE Power & Energy Society General Meeting*, pp. 1–5.

[14] X. Liu,"An optimization model for combined heat and power dispatch with short-term forecasted wind power," in *Proc. 2015 IEEE Power & Energy Society General Meeting*, pp. 1–5.

[15] S. Huang, Q. Wu, S. S. Oren, R. Li, and Z. Liu,"Distribution locational marginal pricing through quadratic programming for congestion management in distribution networks," *IEEE Trans. Power Syst.*, vol.30, no.4, pp. 2170–2178, Jul. 2015.

[16] A. Benonysson, B. Bøhm, and H. F. Ravn,"Operational optimization in a district heating system," *Energy Convers. Manag.*, vol.36, no.5, pp. 297–314, May 1995.

[17] Z. Li, W. Wu, M. Shahidehpour, J. Wang, and B. Zhang,"Combined Heat and Power Dispatch Considering Pipeline Energy Storage of District Heating Network," *IEEE Trans. Sustain. Energy*, vol.7, no.1, pp. 12–22, Jan. 2016.

[18] J. Li, J. Fang, Q. Zeng, and Z. Chen,"Optimal operation of the integrated electrical and heating systems to accommodate the intermittent renewable sources," *Appl. Energy*, vol.167, pp. 244–254, Apr. 2016.

[19] Z. Pan, Q. Guo, and H. Sun,"Feasible region method based integrated heat and electricity dispatch considering building thermal inertia," *Appl. Energy*, vol.192, pp. 395–407, Apr. 2017.

[20] B. van der Heijde, M. Fuchs, C. Ribas Tugores, G. Schweiger, K. Sartor, D. Basciotti, D. Müller, C. Nytsch-Geusen, M. Wetter, and L. Helsen,"Dynamic equation-based thermo-hydraulic pipe model for district heating and cooling systems," *Energy Convers. Manag.*, vol.151, pp. 158–169, Nov. 2017.

[21] S. Brückner, S. Liu, L. Miró, M. Radspieler, L. F. Cabeza, and E. Lävemann,"Industrial waste heat recovery technologies: An economic analysis of heat transformation technologies," *Appl. Energy*, vol.151, pp. 157–167, Aug. 2015.

[22] J. Lofberg,"YALMIP : a toolbox for modeling and optimization in MATLAB," in *Proc. 2004 IEEE International Conference on Robotics and Automation (IEEE Cat. No.04CH37508)*, pp. 284–289.

[23] "IBM Knowledge Center - MIQCP: mixed integer programs with quadratic terms in the constraints." Available: https://www.ibm.com/support/knowledgecenter/en/SSSA5P_12.8.0/ilog.odms.cplex.help/CPLEX/U

srMan/topics/discr_optim/mip_quadratic/03_introMIQCP.html. [Accessed: 21-Jan-2019].